TITLE:

Unlocking the Full Potential of Polymer-Based Solid-State Photon Upconversion

AUTHOR(S):

Sakamoto, Yuji; Tamai, Yasunari

CITATION:

Sakamoto, Yuji ...[et al]. Unlocking the Full Potential of Polymer-Based Solid-State Photon Upconversion. ECS Journal of Solid State Science and Technology 2022, 11(12): 121005.

ISSUE DATE:

2022-12

URL:

http://hdl.handle.net/2433/285225

RIGHT:

© 2022 The Author(s). Published on behalf of The Electrochemical Society by IOP Publishing Limited; This is an open access article distributed under the terms of the Creative Commons Attribution 4.0 License (CC BY), which permits unrestricted reuse of the work in any medium, provided the original work is properly cited.

京都大学学術情報リポジトリ
KURENAI 紅
Kyoto University Research Information Repository

京都大学 KYOTO UNIVERSITY
A Self-archived copy in
Kyoto University Research Information Repository
https://repository.kulib.kyoto-u.ac.jp
京都大学学術情報リポジトリ KURENAI 紅 Kyoto University Research Information Repository

ECS Journal of Solid State Science and Technology, 2022 **11** 121005

Unlocking the Full Potential of Polymer-Based Solid-State Photon Upconversion

Yuji Sakamoto[1] **and Yasunari Tamai**[1,2,z]

[1]*Department of Polymer Chemistry, Graduate School of Engineering, Kyoto University, Katsura, Nishikyo, Kyoto 615-8510, Japan*
[2]*Japan Science and Technology Agency (JST), PRESTO, 4-1-8 Honcho Kawaguchi, Saitama 332-0012, Japan*

To harvest the full potential of polymer-based solid-state photon upconversion (UC) devices, we examined the effect of the molecular weight of a fluorescent polymer on the UC efficiency. With a high-molecular-weight polymer, a long triplet lifetime of 11.2 ms was achieved, which led to a characteristic threshold intensity of 67 mW cm^{-2}, considerably lower than those of previously reported polymer-based UC devices. Furthermore, the external quantum efficiency of our UC device was as high as ~0.35%. Consequently, fluorescent conjugated polymers with long triplet lifetimes can serve as attractive candidates for efficient solid-state UC devices.

© 2022 The Author(s). Published on behalf of The Electrochemical Society by IOP Publishing Limited. This is an open access article distributed under the terms of the Creative Commons Attribution 4.0 License (CC BY, http://creativecommons.org/licenses/by/4.0/), which permits unrestricted reuse of the work in any medium, provided the original work is properly cited. [DOI: 10.1149/2162-8777/acab84]

Manuscript submitted August 16, 2022; revised manuscript received December 2, 2022. Published December 21, 2022. *This paper is part of the JSS Focus Issue on ECS Nano: Early Career Researchers.*

Supplementary material for this article is available online

Photon upconversion (UC), a photophysical reaction that converts longer-wavelength input light into a shorter-wavelength emission,[1–10] has been recently gained significant attention owing to its potential applications in various fields, including solar cells, artificial photosynthesis, and bioimaging.[5,11–14] UC based on triplet–triplet annihilation (TTA-UC) begins with the absorption of a low-energy photon by a triplet sensitizer (TS) to form a singlet exciton, followed by intersystem crossing to form a triplet exciton, which is subsequently transferred to an emitter with low-lying triplet- and high-lying singlet-state energy levels. The triplet exciton then randomly diffuses and undergoes TTA upon meeting another emitter triplet, resulting in the formation of a high-energy emitter singlet, followed by UC emission. The internal and external quantum yields (QYs) of the UC emission (Φ_{UC} and EQE, respectively) and the characteristic threshold intensity I_{th}, above which Φ_{UC} and EQE approach their maximum values, are the primary indicators of the UC efficiency. A high UC QY is crucial for the practical application of UC devices. Note that the internal QY (Φ_{UC}) is defined as the ratio between the number of *absorbed* and emitted photons, while the external QY (EQE) is defined as the ratio between the number of *irradiated* and emitted photons. Therefore, EQE is, in principle, more important than Φ_{UC} for the practical application of UC devices. On the other hand, a low I_{th} is also critical as a maximum QY can be obtained with a weak excitation intensity.

Small molecular fluorescent materials, such as 9,10-diphenylanthracene, are commonly employed as emitters. In contrast, conjugated polymers are attractive candidates as emitters for solid-state UC devices owing to their facile thin-film fabrication via wet processes. The QYs of polymer-based UC devices are typically lag far behind those of small-molecule-based devices. However, we have previously demonstrated that the EQEs of polymer-based devices can compete with those of small-molecule-based counterparts.[15] In contrast, the remaining challenge for polymer-based devices is their considerably larger I_{th} compared with those of small-molecule-based devices. For instance, we have reported that I_{th} of a polymer-based solid-state UC device consisting of Pt(II)octaethylporphyrin (PtOEP) as a TS and poly[(9,9'-dihexylfluorenyl-2,7-diyl)-*alt*-(9,10-anthracene)] (P(F-An)) as an emitter (Fig. 1) is as large as 570 mW cm^{-2},[15] which is more than one order of magnitude larger than those of relatively well-performing small-molecule-based devices.[8,16,17] I_{th} of greater than several hundreds of mW cm^{-2} has also been previously reported for UC devices based on a conjugated copolymer of spirofluorene and anthracene units.[18]

Herein, we successfully reduced I_{th} of polymer-based UC devices by almost an order of magnitude, wherein a low I_{th} of 67 mW cm^{-2} was obtained. The molecular weight of the conjugated polymers was determined to be crucial for extending the lifetime of triplet excitons. A higher-molecular-weight polymer exhibited a longer triplet lifetime, leading to a lower I_{th}. EQE of the corresponding device was as high as ~0.35%, which is among the highest EQEs reported for polymer-based devices.

Experimental

Sample preparation.—PtOEP (Frontier Scientific, Inc.), P(F-An) (Sigma Aldrich), and anthracene-attached poly(methyl methacrylate) (PMMA-An; Polymer Source, Inc., see Fig. S1) were used as received. The weight-averaged molecular weight M_w of P(F-An) was 4.3×10^4, more than twice of that employed in our previous study ($M_w = 1.8 \times 10^4$). Thin films were prepared on quartz substrates by spin-coating from chloroform solutions. Unless otherwise noted, the blend ratio of PtOEP:P(F-An) binary blend films was 1:19 by weight, whereas that of PtOEP:PMMA-An:P(F-An) ternary blend films was 1:18:1 by weight. The sample films were encapsulated in a N_2-purged glovebox for transient absorption (TA) and photoluminescence (PL) measurements.

Measurements

UV–visible absorption and PL spectra were acquired on a UV–visible spectrometer (Hitachi, U-4100) and a PL spectrometer (Horiba Jobin Yvon, Nanolog) equipped with a photomultiplier tube (Hamamatsu, R928P), respectively. A xenon lamp with a monochromator was used as the weak excitation source. The UC emission spectra were recorded using a spectrometer (ANDOR, Shamrock 500i) equipped with a CCD camera (ANDOR, iDus DU420A-BEX2-DD). A 532 nm CW laser (RGB photonics, λ beam 532–200 DPSS) was used as the high-power excitation source. The relative Φ_{UC} was calculated relative to that of pristine PtOEP doped in a polystyrene (PS) film, as follows[13,19]

$$\Phi_{UC} = \Phi_{std}\left(\frac{1-10^{-A_{std}}}{1-10^{-A_{UC}}}\right)\left(\frac{I_{UC}}{I_{std}}\right)\left(\frac{P_{std}}{P_{UC}}\right)\left(\frac{n_{UC}}{n_{std}}\right)^2 \quad [1]$$

where A, I, P, and n are the absorbance at the excitation wavelength, integrated PL intensity, excitation intensity, and refractive index of the medium, respectively. The subscript "std" refers to the standard

[z]E-mail: tamai@photo.polym.kyoto-u.ac.jp

京都大学 KYOTO UNIVERSITY
A Self-archived copy in
Kyoto University Research Information Repository
https://repository.kulib.kyoto-u.ac.jp
京都大学学術情報リポジトリ KURENAI 紅 Kyoto University Research Information Repository

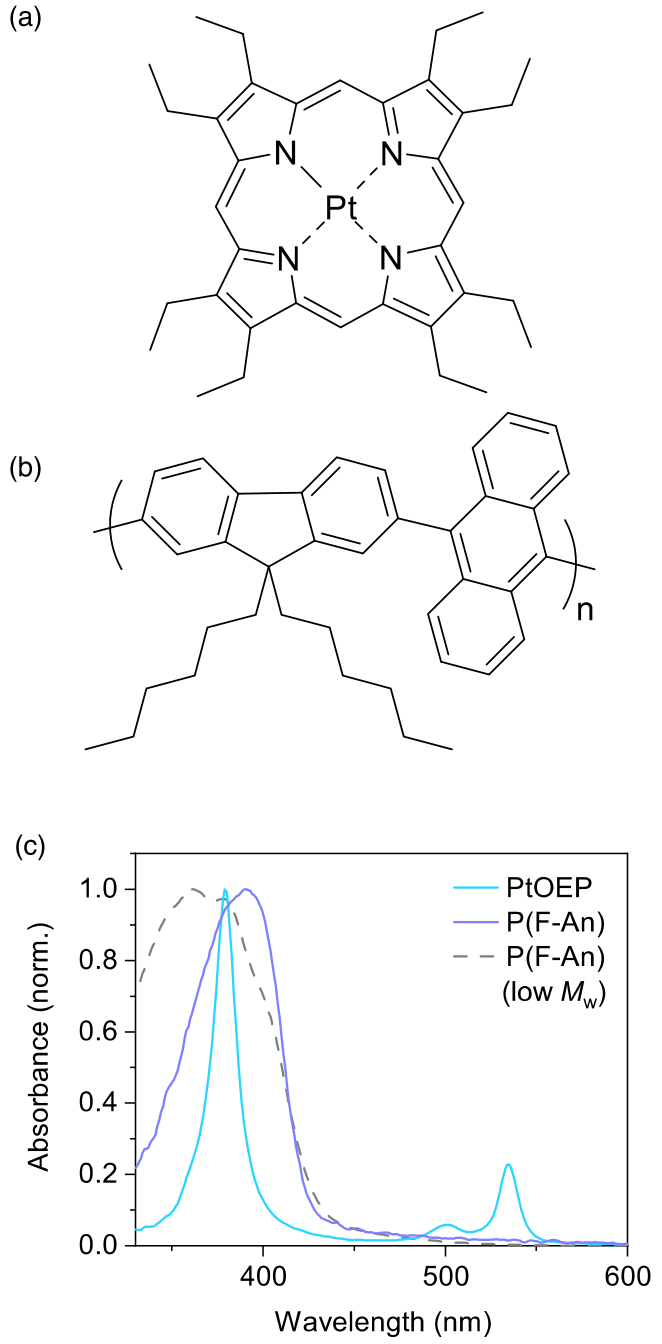

Figure 1. Chemical structures of (a) POEP, and (b) P(F-An). (c) Normalized absorption spectra of PtOEP dispersed in PMMA matrix and a pristine P(F-An) film. The dashed line represents the absorption spectrum of the lower M_w P(F-An) obtained from Ref.15.

PtOEP:PS film. The refractive indices of P(F-An) and PS were assumed to be 1.75 and 1.59, respectively.[20–22] The PLQY of the standard sample Φ_{std} was determined with an integrating sphere using an absolute QY measuring system (Bunko-keiki, BEL-300). EQE is defined as EQE = $\Phi_{UC} \times (1-10^{-A})$.

The TA data were collected using a highly sensitive microsecond TA system.[23] A Nd:YAG laser (Elforlight, SPOT-10–200–532) emitting 532 nm light was used as the excitation source. White light from a tungsten lamp with a stabilized power source was used as the probe light. Two monochromators and appropriate optical cut-off filters were placed before and after the sample to increase the signal-to-noise ratio.

Results and Discussion

Figure 1c shows the normalized absorption spectra of PtOEP dispersed in a thin film of PMMA and a pristine P(F-An) film. Interestingly, the absorption maximum of the higher M_w P(F-An) employed in this study was redshifted and the bandwidth of the absorption spectrum was narrower as compared with those of the lower M_w P(F-An). These results indicate a lower degree of energetic disorder in the higher M_w P(F-An) compared to the lower M_w P(F-An) probably owing to the reduced terminal group effect, resulting in a more coplanar conformation in thin films.

Figure S2 shows the absorption and PL spectra of a PtOEP:P(F-An) binary blend film as well as PtOEP-doped PMMA film after photoexcitation at 532 nm to selectively excite PtOEP.[24,25] Both films exhibited a sharp PtOEP phosphorescence band at ~645 nm.[24–26] However, the PL intensity of the PtOEP:P(F-An) blend film was significantly lower than that of the PtOEP:PMMA blend film, indicating triplet energy transfer (TET) from PtOEP to P(F-An). The QY of TET Φ_{TET} from PtOEP to P(F-An) was determined to be 76% based on the phosphorescence intensity ratio (see Fig. S3 and corresponding discussion for more details). Figure 2a shows the TA spectra of the PtOEP:P(F-An) binary blend film. A photo-induced absorption (PIA) band attributable to PtOEP triplets in the 750–800 nm region decayed rapidly (assignments of the TA spectra were detailed in our previous study).[15] Instead, a broad PIA attributable to P(F-An) triplets in the <700 nm region remained over a millisecond time scale. The intrinsic lifetime of P(F-An) triplets was determined from the excitation-intensity-independent triplet decay kinetics (Fig. 2b), where the contribution of TTA is negligible.[27,28] Notably, the triplet lifetime of the higher M_w P(F-An) was 11.2 ms, considerably longer than that of the lower M_w P(F-An) (0.57 ms).[15] The significant increase in the triplet lifetime is probably associated with the more coplanar conformation owing to the lower level of energetic disorder in the higher M_w P(F-An). This is because a small reorganization energy between the lowest triplet and ground states, owing to a coplanar conformation, is expected to lead to a small nonradiative decay rate of the P(F-An) triplets.[29] As I_{th} is inversely proportional to the square of the triplet lifetime,[4,30] a significant enhancement in the triplet lifetime should result in a reduction in I_{th}.

We next measured UC emission spectra of the PtOEP:P(F-An) binary blend film at various excitation intensities (Fig. 3a) under 532 nm excitation (indicated by the green arrow) to selectively excite PtOEP. The PL response at wavelengths shorter than the excitation source was observed. This PL can be attributable to the UC emission from P(F-An) as the spectral shape is consistent with the fluorescence spectrum of P(F-An), as indicated by the dashed line. As the excitation intensity increased, the UC emission intensity initially increased quadratically and then exhibited a linear dependence at high excitation intensities (Fig. 3b). I_{th}, determined from the intersection of two fitting lines representing the quadratic and linear dependences, was as small as 67 mW cm^{-2}, considerably lower than that obtained in our previous study (570 mW cm^{-2}),[15] owing to the increased triplet lifetime. Further, Φ_{UC} is as high as ~0.6% (out of a maximum of 50%, Fig. 3c), more than one order of magnitude higher than that obtained in our previous study wherein Φ_{UC} was as low as ~0.04%. EQE was as high as ~0.35%, which is also considerably higher than previously reported EQEs of solid-state UC devices wherein EQEs hardly exceeded 0.1%.[15,31–34] One exception was recently reported by Izawa et al.[35,36] wherein an EQE of 2.3% was achieved. However, their device was based on a completely different UC mechanism. Therefore, our UC device exhibits the highest EQE for TS:emitter-based UC systems, indicating that fluorescent conjugated polymers with high molecular weights serve as highly attractive candidates for solid-state UC applications. Note that Φ_{UC} of our device was considerably lower than those of the previously reported well-performing solid-state UC devices owing to the relatively high (5 wt%) blend ratio of PtOEP. A high sensitizer contents cause significant back singlet energy transfer from the

京都大学 KYOTO UNIVERSITY
A Self-archived copy in
Kyoto University Research Information Repository
https://repository.kulib.kyoto-u.ac.jp
京都大学学術情報リポジトリ KURENAI 紅 Kyoto University Research Information Repository

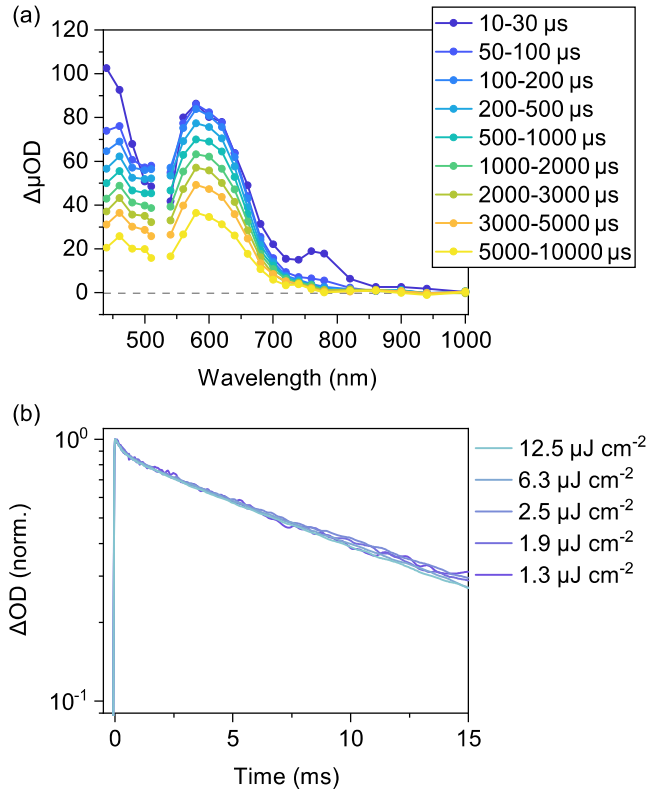

Figure 2. (a) TA spectra of a PtOEP:P(F-An) binary blend film. The excitation wavelength was set to 532 nm with a fluence of 11 μJ cm^{-2}. (b) Time evolution of P(F-An) triplets monitored at 600 nm. The decay kinetics can be fitted with the sum of two exponential functions with time constants of 1.2 ms (15%) and 13.0 ms (85%), yielding an averaged lifetime of 11.2 ms.

emitter to the sensitizer,[31] leading to considerably decresed PLQY of the emitter. We previously observed that Φ_{UC} increases significantly, while EQE decreases, with decreasing the PtOEP blend ratio.[15] As the main aim of this study is to demonstrate the molecular-weight-dependence of the threshold intensity I_{th}, we prioritized improving the signal-to-noise ratios in the TA measurements. A larger PtOEP blend ratio also guarantees the reliability of the Φ_{UC} and EQE values. Simultaneously achieving sufficient light harvesting while suppressing back singlet energy transfer is a major challenge to overcome and beyond the scope of this study.

To realize further improvement in the UC efficiency, we also examined a ternary-blend-based UC device consisting of PtOEP as the TS, PMMA-An as the host,[37] and a small amount of P(F-An) as the emitter, wherein the triplet energies decreases in the order of PtOEP, PMMA-An, and P(F-An) (Fig. S1a).[15,38] The ternary-blend concept was recently introduced by us to improve the UC efficiency. The key idea underpinning this concept involves triplet accumulation in small emitter domains driven by the cascaded triplet energy landscape. At a small emitter blend ratio, the local triplet density in the emitter domain is higher than that averaged over the entire film, which is beneficial for accelerating TTA in the small emitter domains as TTA is a bimolecular reaction. We have previously demonstrated that TTA is accelerated in a ternary blend film owing to the triplet accumulation effect.[15] Figure 4 shows the UC emission spectra of a PtOEP:PMMA-An:P(F-An) ternary blend film; however, contrary to expectations, the UC emission of the ternary blend was weaker than that of the PtOEP:P(F-An) binary blend (Fig. 3).

To unveil the origin of the less efficient UC emission from the ternary blend film, we performed TA measurements for this film. Figure S4 shows the TA spectra of the ternary blend film. The PIA attributable to P(F-An) triplets was also observed in the ternary blend film at later times. However, the signal amplitude of the triplet

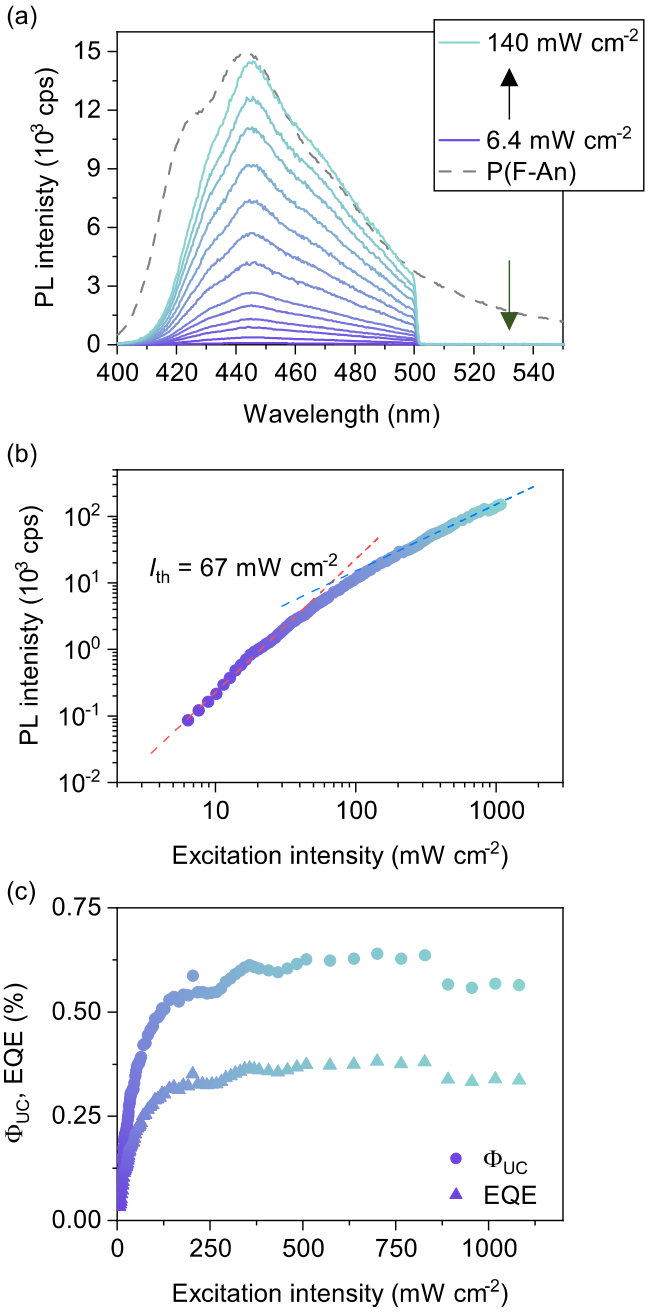

Figure 3. (a) UC emission spectra of a PtOEP:P(F-An) binary blend film excited at 532 nm. The excitation intensity was varied over 6.4–140 mW cm^{-2} from bottom to top. Emission above 500 nm was cut using a short-pass filter. The dashed line represents the fluorescence spectrum of a thin P(F-An) film after photoexcitation at 320 nm. Note that the depression in the 400–440 nm region is attributable to the self-absorption of fluorescence by the P(F-An) itself due to the relatively thick film of our UC device (Figure S2). (b) Log–log plots of UC emission intensity as a function of excitation intensity. The dashed lines represent best fitting curves with slopes of 2 (red) and 1 (blue). I_{th} was determined as the intersection of the two dashed lines. (c) Φ_{UC} and EQE as a function of excitation intensity (out of a maximum of 50%).

PIA was considerably smaller than that of the binary blend, indicating that inefficient TET from PMMA-An to P(F-An) limited the UC efficiency of the ternary blend film. By comparing the initial TA signals of the PtOEP:P(F-An) binary and PtOEP:PMMA-An:P(F-An) ternary blend films, Φ_{TET} from PMMA-An to P(F-An) in the ternary blend film was roughly estimated to be as low as ~11% (Fig. S5). We also found that Φ_{TET} increased monotonically with

京都大学 KYOTO UNIVERSITY
A Self-archived copy in
Kyoto University Research Information Repository
https://repository.kulib.kyoto-u.ac.jp
京都大学学術情報リポジトリ KURENAI 紅 Kyoto University Research Information Repository

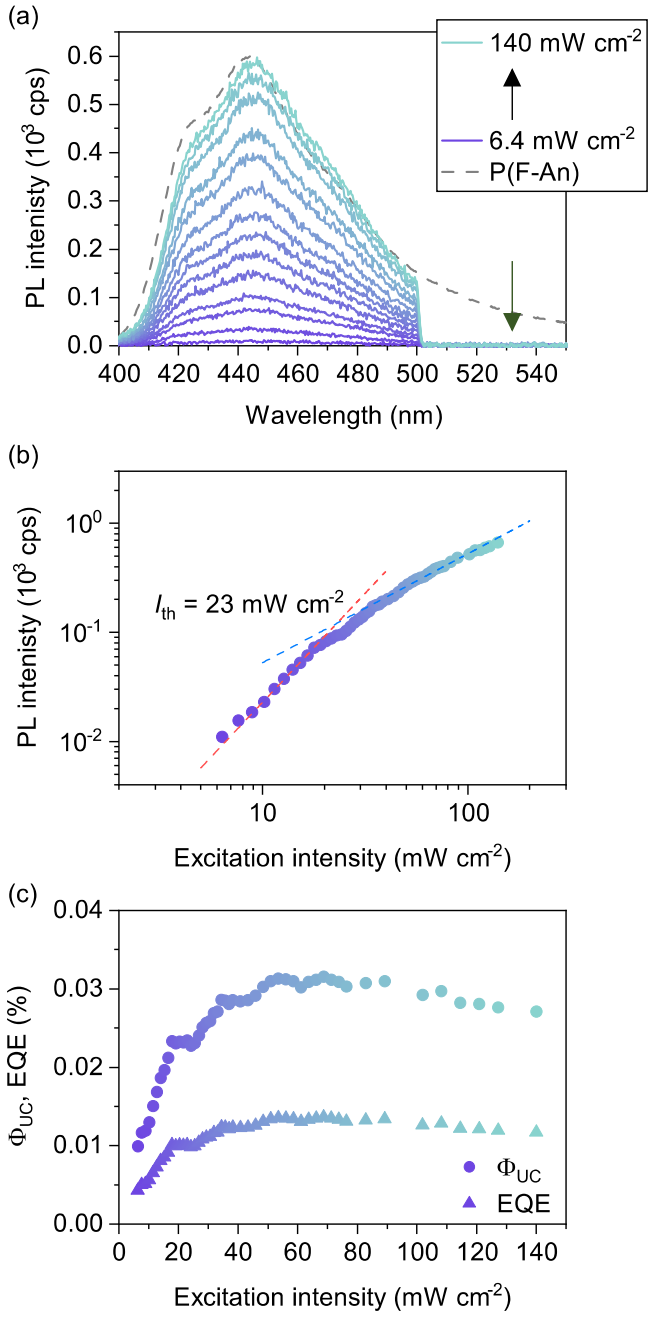

Figure 4. (a) UC emission spectra of a PtOEP:PMMA-An:P(F-An) ternary blend film excited at 532 nm. The excitation intensity was varied over 6.4–140 mW cm^{-2} from bottom to top. Emission above 500 nm was cut using a short-pass filter. The dashed line represents the fluorescence spectrum obtained with a thin P(F-An) film after photoexcitation at 320 nm. (b) Log–log plots of UC emission intensity as a function of excitation intensity. The dashed lines represent fitting curves with slopes of 2 (red) and 1 (blue). I_{th} was determined as the intersection of the two dashed lines. (c) Φ_{UC} and EQE as a function of excitation intensity (out of a maximum of 50%).

increasing blend ratio of P(F-An), indicating that the slow triplet diffusion in the PMMA-An domain limits Φ_{TET} of the ternary blend. The significantly weakened UC emission from the PtOEP:PMMA-An binary blend film confirmed that the triplet exciton diffusion in the PMMA-An film limited the UC efficiency (Fig. S6).

Notably, the decay kinetics of the P(F-An) triplets at early times became faster with decreasing blend ratio of P(F-An), as shown in Fig. S5c. This result indicates that P(F-An) triplets were more likely to decay through TTA in the ternary blend film with a small P(F-An) blend ratio, despite the lower P(F-An) triplet density. That is, TTA was highly accelerated in the ternary blends owing to the triplet accumulation effect. Consequently, I_{th} was reduced to 23 mW cm^{-2} in the ternary blend despite the inefficient TET. This means that if Φ_{TET} from the host to the emitter is increased to 100%, which has been achieved in our previous study, I_{th} can decrease to ~3 mW cm^{-2}, which is comparable to the intensity of Sunlight in the green light region.

Conclusions

We have examined the molecular-weight-dependence of the emitter polymer on unlocking the full potential of polymer-based solid-state UC devices. The triplet lifetime of the emitter polymer P(F-An) showed a remarkable molecular weight dependence. Upon using a high M_w P(F-An), the triplet lifetime increased significantly to 11.2 ms, which is considerably longer than that of the lower M_w P(F-An) obtained in our previous study (0.57 ms). The long triplet lifetime led to a low I_{th} of 67 mW cm^{-2} for the PtOEP:P(F-An) binary blend, which is considerably lower than those previously reported for polymer-based UC devices. EQE of this device was ~0.35%, which is the highest value ever reported for TS:emitter systems. Therefore, fluorescent conjugated polymers with long triplet lifetimes serve as attractive candidates for efficient solid-state UC devices.

A ternary-blend UC device consisting of PtOEP, PMMA-An, and P(F-An) as the TS, host, and emitter, respectively, exhibited a further reduced I_{th} of 23 mW cm^{-2} owing to the triplet accumulation effect even though the UC efficiency of the ternary blend lagged behind that of the PtOEP:P(F-An) binary blend due to the low TET yield from PMMA-An to P(F-An). This result indicates that if the TET yield is improved, the UC efficiency would improve significantly. Based on our estimation, the ternary blend concept has the potential to reduce I_{th} by up to a few mW cm^{-2} if a near-unity TET yield can be achieved.

Acknowledgments

This study was partly supported by the JST PRESTO program Grant Number JPMJPR1874, and JSPS KAKENHI Grant Numbers 21H02012, 21H05394, and 22K19065.

ORCID

Yasunari Tamai https://orcid.org/0000-0002-3074-0208

References

1. A. Köhler and H. Bässler, *Mater. Sci. Eng. R Rep.*, **66**, 71 (2009).
2. T. N. Singh-Rachford and F. N. Castellano, *Coord. Chem. Rev.*, **254**, 2560 (2010).
3. Y. C. Simon and C. Weder, *J. Mater. Chem.*, **22**, 20817 (2012).
4. A. Monguzzi, R. Tubino, S. Hoseinkhani, M. Campione, and F. Meinardi, *Phys. Chem. Chem. Phys.*, **14**, 4322 (2012).
5. J. Zhou, Q. Liu, W. Feng, Y. Sun, and F. Li, *Chem. Rev.*, **115**, 395 (2015).
6. N. Yanai and N. Kimizuka, *Chem. Commun.*, **52**, 5354 (2016).
7. N. Yanai and N. Kimizuka, *Acc. Chem. Res.*, **50**, 2487 (2017).
8. V. Gray, K. Moth-Poulsen, B. Albinsson, and M. Abrahamsson, *Coord. Chem. Rev.*, **362**, 54 (2018).
9. B. Joarder, N. Yanai, and N. Kimizuka, *J. Phys. Chem. Lett.*, **9**, 4613 (2018).
10. A. Ronchi and A. Monguzzi, *Chem. Phys. Rev.*, **3**, 041301 (2022).
11. T. F. Schulze and T. W. Schmidt, *Energy Environ. Sci.*, **8**, 103 (2015).
12. X. Zhu, Q. Su, W. Feng, and F. Li, *Chem. Soc. Rev.*, **46**, 1025 (2017).
13. Y. Tamai, *Aggregate in press*, (2022).
14. Y. Tamai, *Adv. Energy Sustainability Res. in press* (2022).
15. Y. Sakamoto, Y. Tamai, and H. Ohkita, *J. Chem. Phys.*, **153**, 161102 (2020).
16. M. Hosoyamada, N. Yanai, T. Ogawa, and N. Kimizuka, *Chem. Eur. J.*, **22**, 2060 (2016).
17. R. Enomoto, M. Hoshi, H. Oyama, H. Agata, S. Kurokawa, H. Kuma, H. Uekusa, and Y. Murakami, *Mater. Horizons*, **8**, 3449 (2021).
18. F. Laquai, G. Wegner, C. Im, A. Büsing, and S. Heun, *J. Chem. Phys.*, **123**, 074902 (2005).
19. N. Yanai, K. Suzuki, T. Ogawa, Y. Sasaki, N. Harada, and N. Kimizuka, *J. Phys. Chem. A*, **123**, 10197 (2019).
20. H. Azuma, T. Kobayashi, Y. Shim, N. Mamedov, and H. Naito, *Org. Electron.*, **8**, 184 (2007).

京都大学 KYOTO UNIVERSITY
A Self-archived copy in
Kyoto University Research Information Repository
https://repository.kulib.kyoto-u.ac.jp
京都大学学術情報リポジトリ KURENAI 紅 Kyoto University Research Information Repository

21. M. Campoy-Quiles, G. Heliotis, R. Xia, M. Ariu, M. Pintani, P. Etchegoin, and D. D. C. Bradley, *Adv. Funct. Mater.*, **15**, 925 (2005).
22. P. O. Morawska et al., *J. Phys. Chem. C*, **119**, 22102 (2015).
23. H. Ohkita, Y. Tamai, H. Benten, and S. Ito, *IEEE J. Sel. Top. Quantum Electron.*, **22**, 100 (2016).
24. Y. V. Aulin, M. van Sebille, M. Moes, and F. C. Grozema, *RSC Adv.*, **5**, 107896 (2015).
25. A. K. Bansal, W. Holzer, A. Penzkofer, and T. Tsuboi, *Chem. Phys.*, **330**, 118 (2006).
26. G. Klärner, M. H. Davey, W.-D. Chen, J. C. Scott, and R. D. Miller, *Adv. Mater.*, **10**, 993 (1998).
27. Y. Tamai, H. Ohkita, H. Benten, and S. Ito, *Chem. Mater.*, **26**, 2733 (2014).
28. S. Mattiello, S. Mecca, A. Ronchi, A. Calascibetta, G. Mattioli, F. Pallini, F. Meinardi, L. Beverina, and A. Monguzzi, *ACS Energy Lett.*, **7**, 2435 (2022).
29. A. Monguzzi, J. Mezyk, F. Scotognella, R. Tubino, and F. Meinardi, *Phys. Rev. B*, **78**, 195112 (2008).
30. R. Englman and J. Jortner, *Mol. Phys.*, **18**, 145 (1970).
31. T. Ogawa, M. Hosoyamada, B. Yurash, T.-Q. Nguyen, N. Yanai, and N. Kimizuka, *J. Am. Chem. Soc.*, **140**, 8788 (2018).
32. M. Wu, D. N. Congreve, M. W. B. Wilson, J. Jean, N. Geva, M. Welborn, T. Van Voorhis, V. Bulović, M. G. Bawendi, and M. A. Baldo, *Nat. Photonics*, **10**, 31 (2016).
33. A. Abulikemu, Y. Sakagami, C. Heck, K. Kamada, H. Sotome, H. Miyasaka, D. Kuzuhara, and H. Yamada, *ACS Appl. Mater. Interfaces*, **11**, 20812 (2019).
34. T.-A. Lin, C. F. Perkinson, and M. A. Baldo, *Adv. Mater.*, **32**, 1908175 (2020).
35. S. Izawa and M. Hiramoto, *Nat. Photonics*, **15**, 895 (2021).
36. Y. Sakamoto, S. Izawa, H. Ohkita, M. Hiramoto, and Y. Tamai, *Commun. Mater.*, **3**, 76 (2022).
37. X. Yu, X. Cao, X. Chen, N. Ayres, and P. Zhang, *Chem. Commun.*, **51**, 588 (2015).
38. S. Reineke and M. A. Baldo, *Sci. Rep.*, **4**, 3797 (2014).